AEM
Journals.ASM.org

Metabolic Engineering of *Corynebacterium glutamicum* for Methanol Metabolism

Sabrina Witthoff, Katja Schmitz, Sebastian Niedenführ, Katharina Nöh, Stephan Noack, Michael Bott, Jan Marienhagen

Institute of Bio- and Geosciences, IBG-1: Biotechnology, Forschungszentrum Jülich, Jülich, Germany

Methanol is already an important carbon feedstock in the chemical industry, but it has found only limited application in biotechnological production processes. This can be mostly attributed to the inability of most microbial platform organisms to utilize methanol as a carbon and energy source. With the aim to turn methanol into a suitable feedstock for microbial production processes, we engineered the industrially important but nonmethylotrophic bacterium *Corynebacterium glutamicum* toward the utilization of methanol as an auxiliary carbon source in a sugar-based medium. Initial oxidation of methanol to formaldehyde was achieved by heterologous expression of a methanol dehydrogenase from *Bacillus methanolicus*, whereas assimilation of formaldehyde was realized by implementing the two key enzymes of the ribulose monophosphate pathway of *Bacillus subtilis*: 3-hexulose-6-phosphate synthase and 6-phospho-3-hexuloisomerase. The recombinant *C. glutamicum* strain showed an average methanol consumption rate of 1.7 ± 0.3 mM/h (mean ± standard deviation) in a glucose-methanol medium, and the culture grew to a higher cell density than in medium without methanol. In addition, [^{13}C]methanol-labeling experiments revealed labeling fractions of 3 to 10% in the m + 1 mass isotopomers of various intracellular metabolites. In the background of a *C. glutamicum* Δ*ald* Δ*adhE* mutant being strongly impaired in its ability to oxidize formaldehyde to CO_2, the m + 1 labeling of these intermediates was increased (8 to 25%), pointing toward higher formaldehyde assimilation capabilities of this strain. The engineered *C. glutamicum* strains represent a promising starting point for the development of sugar-based biotechnological production processes using methanol as an auxiliary substrate.

Highly productive strains of *Corynebacterium glutamicum* have been developed to produce several million tons of amino acids annually, in particular the feed additive L-lysine and the flavor enhancer L-glutamate. In addition, extensive research has focused on engineering *C. glutamicum* for the microbial production of a variety of other commercially interesting compounds (1), such as organic acids (2–4), diamines (5–7), and alcohols (8–10). The natural substrate spectrum of *C. glutamicum* includes sugars, organic acids, and alcohols, but for industrial production processes mainly glucose (from starch) or sucrose and fructose (from molasses) are used as carbon sources (11–13). The availability and price of sugars are influenced by seasonal variations and weather conditions and are also subject to price regulations and import limitations imposed on agricultural products. Furthermore, due to the increasing world population and loss of arable land, the sugar price is expected to rise in the coming decades. Thus, there is demand for an alternative carbon source for the microbial production of valuable compounds (14). In recent years, *C. glutamicum* has been genetically engineered toward the ability to efficiently utilize several cheap carbon sources, such as the tricarboxylic acid cycle intermediates malate, fumarate, and succinate and the lignocellulosic compounds arabinose and xylose, as well as starch, cellobiose, glycerol, lactose, galactose, and glucosamine (references 11 and 15 and references therein). Cheap raw methanol that may contain impurities, such as ethanol, higher alcohols, or water, is already an important carbon feedstock in the chemical industry and also represents an interesting alternative substrate. At present, methanol is mainly produced from synthesis gas (a mixture of CO and H_2), which is obtained by catalytic reforming of coal or natural gas. In addition, procedures are available for producing methanol from renewable carbon sources (16–19). The high availability and low market price of methanol raise the question of whether this C_1 compound could also serve as alternative carbon source for microbial production processes (20, 21). Although *C. glutamicum* harbors an endogenous pathway for oxidation of methanol to CO_2 (22, 23), it is a nonmethylotrophic organism and therefore is not able to utilize C_1 compounds as the sole carbon and energy source.

A key step in methylotrophic metabolism is the oxidation of methanol to formaldehyde. Whereas Gram-negative methylotrophic bacteria such as *Methylobacterium extorquens* employ pyrroloquinoline quinone (PQQ)-dependent and periplasmic methanol dehydrogenases (MDHs) to oxidize methanol (24), Gram-positive thermotolerant *Bacillus* strains usually use NAD^+-dependent cytoplasmic methanol dehydrogenases (25). The cytotoxic formaldehyde is either assimilated into cell material or further oxidized to carbon dioxide (26, 27). The assimilation of C_1 compounds in methylotrophic bacteria occurs either via the ribulose monophosphate (RuMP) pathway, the serine cycle, or the Calvin-Benson-Bassham cycle. Whereas CO_2 is reduced and converted to biomass in the Calvin-Benson-Bassham cycle, assimilation of carbon in the serine cycle occurs at the level of methylene-

Received 22 September 2014 **Accepted** 12 January 2015

Accepted manuscript posted online 16 January 2015

Citation Witthoff S, Schmitz K, Niedenführ S, Nöh K, Noack S, Bott M, Marienhagen J. 2015. Metabolic engineering of *Corynebacterium glutamicum* for methanol metabolism. Appl Environ Microbiol 81:2215–2225. doi:10.1128/AEM.03110-14.

Editor: A. M. Spormann

Address correspondence to Jan Marienhagen, j.marienhagen@fz-juelich.de.

Supplemental material for this article may be found at http://dx.doi.org/10.1128/AEM.03110-14.

Copyright © 2015, American Society for Microbiology. All Rights Reserved.

doi:10.1128/AEM.03110-14

Downloaded from http://aem.asm.org/ on November 19, 2019 by guest

TABLE 1 Strains and plasmids used in this study

Strain or plasmid	Relevant characteristics	Source or reference
E. coli DH5α	F$^-$ ϕ80d*lac*Δ(*lacZ*)M15 Δ(*lacZYA-argF*) *U169 endA1 recA1 hsdR17*(r_K^- m_K^+) *deoR thi-1 phoA supE44* λ$^-$ *gyrA96 relA1*	Invitrogen (Karlsruhe, Germany)
B. subtilis 168	Wild type, *trpC2*, auxotrophic for tryptophan	BGSC[a]
C. glutamicum strains		
ATCC 13032	Biotin auxotroph, wild-type strain	36
Δ*ald* Δ*adhE*	Derivative of ATCC 13032 with in-frame deletion of *ald* (cg3096) and *adhE* (cg0387)	22
Plasmids		
pEKEx2	Kan^r; *C. glutamicum-E. coli* shuttle vector for regulated gene expression; P_{tac}, *lacI*^{q} pBL1 *ori*V_{Cg} pUC18 *ori*V_{Ec}	37
pVWEx2	Tet^r; *C. glutamicum-E. coli* shuttle vector for regulated gene expression; P_{tac}, *lacI*^{q} pCG1 *ori*V_{Cg} pUC18 *ori*V_{Ec}	38
pVWEx2-Bm(*mdh-act*)	Tet^r; pVWEx2 derivative containing Bm(*mdh-act*) under control of P*tac*	This work
pVWEx2-P*tuf*-Bm(*mdh-act*)	Tet^r; pVWEx2 derivative containing Bm(*mdh-act*) under control of P*tuf*	This work
pVWEx2-Bm(*mdh3-act*)	Tet^r; pVWEx2 derivative containing Bm(*mdh3-act*) under control of P*tac*	This work
pVWEx2-P*tuf*-Bm(*mdh3-act*)	Tet^r; pVWEx2 derivative containing Bm(*mdh3-act*) under control of P*tuf*	This work
pVWEx2-Cg*adhA*	Tet^r; pVWEx2 derivative containing Cg*adhA* under control of P*tac*	This work
pEKEx2-Bs(*hps-phi*)	Kan^r; pEKEx2 derivative containing Bs(*hps-phi*) under control of P*tac*	This work
pEKEx2- P*tuf* -Bs(*hps-phi*)	Kan^r; pEKEx2 derivative containing Bs(*hps-phi*) under control of P*tuf*	This work
pEKEx2-Mg(*hps-phi*)	Kan^r; pEKEx2 derivative containing Mg(*hps-phi*) under control of P*tac*	This work

[a] BGSC, Bacillus Genetic Stock Center.

H_4F and CO_2 (28). In the RuMP pathway, formaldehyde and ribulose-5-phosphate are condensed to form D-arabino-3-hexulose-6-phosphate, which can be isomerized to fructose-6-phosphate. These reactions are catalyzed by 3-hexulose-6-phosphate synthase (HPS) and 6-phosphate-3-hexuloisomerase (PHI), respectively. Fructose-6-phosphate can be converted to pyruvate via glycolysis or the Entner-Doudoroff pathway, or it can be used to regenerate the formaldehyde acceptor ribulose-5-phosphate by utilizing several reactions of the pentose phosphate pathway (29).

In this work, we describe the functional implementation of methanol oxidation and formaldehyde assimilation via the RuMP pathway in *C. glutamicum* and present promising approaches to use methanol as an auxiliary substrate during growth in sugar-based defined medium.

MATERIALS AND METHODS

Bacterial strains, plasmids, media, and growth conditions. Bacterial strains and plasmids used or constructed in the course of this work are listed in Table 1. *C. glutamicum* was routinely cultivated aerobically in either 500-ml baffled shake flasks with 50 ml medium on a rotary shaker (120 rpm) at 30°C or in 48-well FlowerPlates (m2p-labs, Aachen, Germany) filled with 750 μl medium in a BioLectorBasic apparatus (m2p-labs, Aachen, Germany) at 900 rpm, 30°C, and 80% humidity. Growth in shake flasks was monitored by measuring the optical density at 600 nm (OD_{600}), and growth in the BioLectorBasic was monitored online by measuring the backscatter (BS) at 620 nm (gain, 12). The gravimetric determination of cell dry weight (CDW) was performed in triplicate by centrifugation of 2 ml culture broth in predried and preweighed 2-ml Eppendorf tubes. The pelleted cells were dried for 48 h at 80°C and weighed afterwards. LB medium (30) was used for 5-ml precultures, and main cultures were grown in modified CGXII defined medium (31) containing 55 mM glucose. Methanol was added to the culture medium to a final concentration of 120 mM. For strain construction and maintenance, either LB or BHIS agar plates (brain heart infusion [BHI] agar [Difco, Detroit, MI, USA] supplemented with 0.5 M sorbitol) were used. *Escherichia coli* DH5α was used for cloning purposes and was grown aerobically on a rotary shaker (170 rpm) at 37°C in 5 ml LB medium or on LB agar plates (LB medium with 1.8% [wt/vol] agar). If appropriate, kanamycin and/or tetracycline was added to final concentrations of 25 μg ml^{-1} or 5 μg ml^{-1}, respectively (*C. glutamicum*) or 50 μg ml^{-1} or 12.5 μg ml^{-1} (*E. coli*). Correlations between BS values and the CDW were determined by using the following calibration model formula (32, 33): CDW (g liter^{-1}) = 0.048 g liter^{-1} × BS − 0.78 g liter^{-1}.

Strain construction. The enzymes for recombinant DNA work were obtained from Fermentas (St. Leon-Rot, Germany) and Merck Millipore (Billerica, MA, USA). *E. coli* was transformed by using the RbCl method (34), and *C. glutamicum* ATCC 13032 was transformed via electroporation (35). Routine methods, like PCR, restriction, and ligation, were carried out according to standard protocols (30). The oligonucleotides used for cloning were obtained from Eurofins MWG Operon (Ebersberg, Germany) and are listed in Table S1 in the supplemental material. The genes *mdh*, *mdh3*, and *act*, originating from *Bacillus methanolicus* MGA3 (ATCC 53907; NCBI gene accession numbers EIJ77596, EIJ80770, and AAM98772, respectively) were optimized for expression in *C. glutamicum* by adapting the gene sequence to the codon usage of *C. glutamicum*. These genes, as well as the wild-type coding sequence of the operon consisting of *rmpA* (here *hps*) and *rmpB* (here *phi*) from *M. gastri* (NCBI gene accession numbers Q9LBW4 and Q9LBW5, respectively) were ordered from Life Technologies GmbH (Darmstadt, Germany). All genes, synthesized with desired restriction sites for subcloning into *C. glutamicum* expression vectors, were provided as purified DNA on standard vectors (Life Technologies). The *adhA* gene (cg3107) was amplified from genomic DNA of *C. glutamicum* ATCC 13032 by PCR. The genes *yckG* (here *hps*) and *yckF* (here *phi*) were amplified from genomic DNA of *Bacillus subtilis* 168 by PCR. For heterologous gene expression under the control of a constitutive promoter, P*tuf* (promoter of the elongation factor Tu) was first amplified by PCR from genomic DNA of *C. glutamicum* (14 bp to 179 bp upstream of the *tuf* start codon) and subsequently cloned in front of the above-mentioned genes. The correct DNA sequences were verified by DNA sequencing using plasmid-specific primers. Detailed cloning procedures of the constructed vectors are described in the supplemental material.

Determination of methanol and glucose. The quantitative measurement of methanol and glucose in the cell-free supernatant of *C. glutamicum* cultures was performed by capillary gas chromatography (GC) using an Agilent 7890A gas chromatograph (Agilent Technologies, Waldbronn,

Downloaded from http://aem.asm.org/ on November 19, 2019 by guest

Germany) and by high-performance liquid chromatography (HPLC) analysis using an Agilent 1100 HPLC system (Agilent Technologies, Waldbronn, Germany), respectively, as described previously (22, 39).

Enzyme assays of crude extracts. Recombinant *C. glutamicum* strains were cultivated in 100 ml CGXII defined medium with 55 mM glucose and 120 mM methanol at 30°C and 120 rpm in shake flasks. Induction of gene expression was performed with 1.5 mM isopropyl-β-D-thiogalactopyranoside (IPTG) at an OD_{600} of 1.0. For the determination of enzyme activities in the exponential phase and in the second growth phase, 50 ml of the cell culture was harvested when the OD_{600} reached 5 and 30 ml was harvested after 12 h of cultivation by centrifugation (4,500 × *g*, 15 min, 4°C). Cells were washed with 100 mM glycine-KOH buffer, pH 9.4 (for the Mdh/Mdh3 enzyme assay) or with 50 mM potassium phosphate buffer, pH 7.6, containing 1 mM dithiothreitol and 3 mM $MgCl_2$ (for the HPS/PHI enzyme assays). The cell pellets from the exponential phase and the second growth phase were resuspended in 500 μl and 800 μl buffer, respectively. For crude cell extract preparation, mechanical lysis of cells was performed with glass beads (diameter, 0.1 mm; 350 mg in a 1.5-ml screw-cap tube) for three times, 20 s each, using the Precellys24 apparatus (Bertin Technologies, Montigny-le-Bretonneux, France) and centrifuged for 30 min at 4°C and 16.000 × *g* to remove the cell debris. The supernatant was used for the enzyme assays. The enzyme assays were performed in 96-well plates in 200-μl scale at 30°C by following the increase in absorption at 340 nm with the Infinite M200 Pro instrument (Tecan Group AG, Männedorf, Switzerland). The protein concentration of the cell extracts was determined by the method of Bradford (40) using bovine serum albumin as the standard.

The methanol dehydrogenase assay was performed as described previously (41) with slight modifications. The assay mixtures contained 100 mM glycine-KOH buffer, pH 9.4, 5 mM $MgSO_4$, 1 mM dithiothreitol, 1 mM NAD^+, and 40 μl cell extract at different dilutions. The reaction was initiated by the addition of 500 mM methanol and monitored over 3 min. One unit of methanol dehydrogenase activity was defined as the reduction of 1 μmol NAD^+ to NADH per minute.

The coupled HPS/PHI assay was performed as described previously (42), but with minor modifications of the protocol. Briefly, determination of HPS/PHI activities through measurement of NADPH formation requires the activity of three additional enzymes in the assay mixture: phosphoriboisomerase (PRI), phosphoglucoisomerase (PGI), and glucose-6-phosphate dehydrogenase (G6PDH). The assay mixtures contained 50 mM potassium phosphate buffer, pH 7.6, 5 mM $MgCl_2$, 5 mM ribose-5-phosphate, 2.5 mM $NADP^+$, 5 U PGI from yeast (Roche Diagnostics Deutschland GmbH, Mannheim, Germany), 5 U G6PDH from yeast (grade II; Roche Diagnostics Deutschland GmbH, Mannheim, Germany), 5 U PRI from spinach (type I, partially purified powder; Sigma-Aldrich, St. Louis, MO, USA), and 40 μl cell extract at different dilutions. The reaction mixture was incubated for 5 min at 30°C to ensure equilibrium between ribose-5-phosphate and ribulose-5-phosphate. Subsequently, formaldehyde (37% formaldehyde solution; Sigma-Aldrich, St. Louis, MO, USA) was added to a final concentration of 5 mM to start the reaction. The reaction was monitored for 15 min. One unit of coupled HPS/PHI activity was defined as the reduction of 1 μmol $NADP^+$ to NADPH per minute.

Determination of intracellular formaldehyde. Recombinant *C. glutamicum* strains were cultivated in 100 ml CGXII defined medium with 55 mM glucose and 120 mM methanol at 30°C and 120 rpm in shake flasks. Sampling in the exponential and second growth phases as well as mechanical cell lysis and crude cell extract preparation were performed as described above in "Enzyme assays of crude extracts." The crude cell extract was analyzed for formaldehyde content via an enzymatic assay described by Nudelman et al. (43).

Determination of ^{13}C-labeled intracellular metabolites and $^{13}CO_2$. The assimilation of methanol in recombinant *C. glutamicum* strains was monitored in [^{13}C]methanol-labeling experiments. Cells were cultivated in 200 ml CGXII defined medium with 55 mM glucose and 120 mM ^{13}C-labeled methanol (99% atom enrichment; Sigma-Aldrich, St. Louis, MO, USA) in a parallel bioreactor system (DASGIP AG, Jülich, Germany). During the cultivation, $^{13}CO_2$ and $^{12}CO_2$ off-gas analysis was performed as described previously (22). Analysis of the ^{13}C-labeled intracellular metabolites was performed in the exponential growth phase, in the transition from the exponential growth phase to the second growth phase, and also 12 h and 24 h after reaching the second growth phase. Quenching of the metabolic activity as well as extraction and analysis of intracellular metabolites were performed as previously described (44). Raw mass spectrometry data were corrected for the contribution of all naturally abundant isotopes as well the isotopic impurity of the tracer by using the software IsoCor (45).

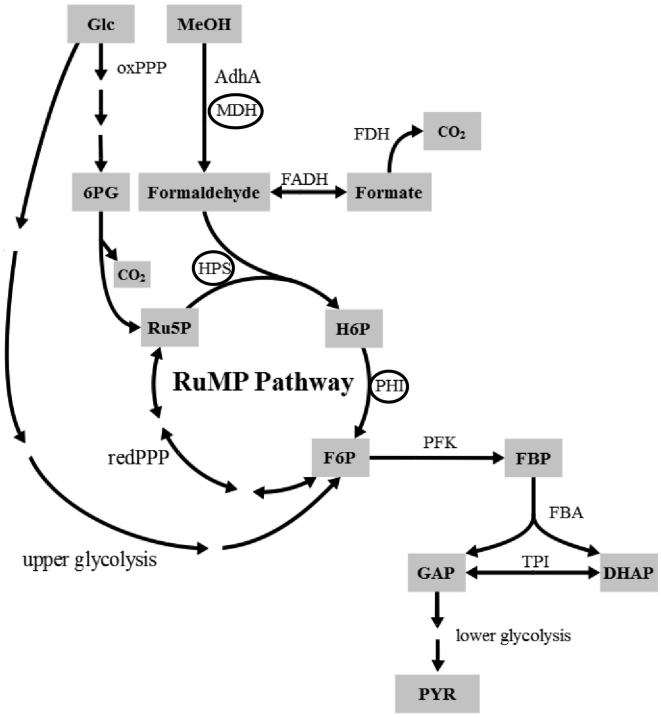

FIG 1 Simplified overview of the (engineered) oxidation of methanol, the endogenous pathway for formaldehyde oxidation, and the synthetic pathway for the assimilation of formaldehyde via the RuMP pathway in the context of the central carbon metabolism of *C. glutamicum*. Abbreviations: oxPPP/redPPP, oxidative/reductive pentose phosphate pathway; MDH, methanol dehydrogenase; AdhA, alcohol dehydrogenase; FADH, formaldehyde dehydrogenase; FDH, formate dehydrogenase; HPS, 3-hexulose-6-phosphate synthase; PHI, 6-phosphate-3-hexuloisomerase; PFK, phosphofructokinase; FBA, fructose bisphosphate aldolase; TPI, triosephosphate isomerase; 6PG, 6-phosphogluconate; Ru5P, ribulose-5-phosphate; H6P, hexulose-6-phosphate; F6P, fructose-6-phosphate; FBP, fructose-1,6-bisphosphate; GAP, glyceraldehyde-3-phosphate; DHAP, dihydroxyacetone phosphate; PYR, pyruvate. The three enzymes (MDH, HPS, and PHI) necessary for establishing a synthetic pathway for methanol oxidation and formaldehyde assimilation in *C. glutamicum* are circled.

RESULTS

Design of a synthetic pathway for the assimilation of methanol-derived carbon in *C. glutamicum*. The first step of engineering *C. glutamicum* toward utilization of methanol was the heterologous expression of a MDHs to oxidize methanol to formaldehyde (Fig. 1). The focus was put on NAD^+-dependent MDHs, since PQQ-dependent MDHs are not suitable for expression in *C. glutamicum*, as this organism does not synthesize PQQ or possess any PQQ-dependent enzymes (46). *B. methanolicus* MGA3 is a well-known methylotroph that harbors three NAD^+-dependent

Downloaded from http://aem.asm.org/ on November 19, 2019 by guest

TABLE 2 Specific activities of Bm(Mdh-Act) and Bm(Mdh3-Act) and coupled specific activities of Bs(Hps-Phi) and Mg(Hps-Phi) in crude cell extracts of *C. glutamicum* strains[a]

Strain	Coupled HPS-PHI sp act (mU/mg) during:		Mdh/Mdh3 sp act (mU/mg) during:	
	Exponential phase	Second growth phase	Exponential phase	Second growth phase
Recombinant *C. glutamicum* strains				
Bm(*mdh-act*) Bs(*hps-phi*)	73.3 ± 24.8	22.1 ± 7.9	0.4 ± 0.2	0.7 ± 0.5
Bm(*mdh-act*) Mg(*hps-phi*)	1.4 ± 1.6	1.0 ± 1.4	ND	ND
P*tuf*-Bm(*mdh-act*) P*tuf*-Bs(*hps-phi*)	53.1 ± 23.5	13.7 ± 1.3	3.3 ± 1.2	2.0 ± 1.5
Recombinant *C. glutamicum* Δ*ald* Δ*adhE* strains				
P*tuf*-Bm(*mdh-act*) P*tuf*-Bs(*hps-phi*)	45.3 ± 9.7	24.3 ± 15.3	5.5 ± 1.1	2.2 ± 1.8
P*tuf*-Bm(*mdh3-act*) P*tuf*-Bs(*hps-phi*)	36.3 ± 4.9	22.3 ± 12.1	6.0 ± 1.5	5.2 ± 1.9
P*tuf*-Bm(*mdh-act*) pEKEx2	ND	ND	5.5 ± 1.1	3.2 ± 2.3

[a] Cells were cultivated in CGXII defined medium with 55 mM glucose and 120 mM methanol at 30°C with shaking at 120 rpm. Genes under the control of P*tac* were induced with 1.5 mM IPTG at an OD_{600} of 1.0. Means and standard deviations were calculated from triplicates, and values were corrected for background activity. The background activity was determined in enzyme assays with the crude cell extracts of *C. glutamicum*(pVWEx2 pEKEx2) and *C. glutamicum* Δ*ald* Δ*adhE*(pVWEx2 pEKEx2). ND, not determined.

MDHs genes (*mdh*, *mdh2*, and *mdh3*) and the MDH activator protein (Act), which modulates the activity of all three MDHs (47, 48). In the presence of Act and with methanol as the substrate, Mdh and Mdh3 shows the highest activity *in vitro* (0.5 U/mg and 0.2 U/mg, respectively), whereas Mdh2 shows the lowest catalytic activity (0.14 U/mg) (48). Thus, genes for *mdh*, *mdh3*, and *act* were codon optimized for expression in *C. glutamicum* and commercially synthesized [Bm(*mdh-act*) and Bm(*mdh3-act*)]. In addition, the AdhA of *C. glutamicum* was previously shown to contribute to endogenous oxidation of methanol to formaldehyde (22). With the aim to simply increase the endogenous methanol oxidation rate, the respective gene (Cg*adhA*) was also chosen as a target for overexpression in *C. glutamicum*.

We decided to pursue the implementation of the RuMP pathway for methanol assimilation in *C. glutamicum* in order to establish that this pathway demands only the functional expression of genes for HPS and PHI. All other enzymatic activities required for the conversion of fructose-6-phosphate and regeneration of ribulose-5-phosphate as a C_1 acceptor can be recruited from the central metabolism of *C. glutamicum* (Fig. 1). Furthermore, these two enzymes require no cofactors, and the assimilation of C_1 via the RuMP pathway occurs directly on the level of formaldehyde and not on the level of methylene-H_4F and/or CO_2, as in the serine cycle (28, 29). Hence, we decided to evaluate the functionality of the HPS and PHI from the nonmethylotroph *B. subtilis* [Bs(*hps-phi*)] and from the methylotroph *Mycobacterium gastri* [Mg(*hps-phi*)] to constitute a functional RuMP pathway in *C. glutamicum*.

Implementation of a synthetic pathway for methanol oxidation and formaldehyde assimilation in wild-type *C. glutamicum*. For growth on methanol, methylotrophic organisms require a pathway for the assimilation of formaldehyde to generate biomass, as well as a pathway for the dissimilation of formaldehyde to generate energy. The dissimilatory pathway also serves as "safety valve" in case of an intracellular accumulation of formaldehyde to toxic amounts. Since the wild-type *C. glutamicum* already possesses an endogenous pathway for the oxidation of naturally occurring cytotoxic formaldehyde to CO_2 (22, 23), we decided to initially express the genes of the synthetic methanol assimilation pathway in this strain. Two plasmids allowing for heterologous gene expression under the control of the IPTG-inducible promoter P*tac* were used: one for the expression of the methanol oxidation modules [Cg*adhA* or Bm(*mdh-act*)] and one for the expression of the formaldehyde assimilation modules [Bs(*hps-phi*) or Mg(*hps-phi*)]. Thus, Cg*adhA* or Bm(*mdh-act*) were individually expressed in combination with Bs(*hps-phi*) or Mg(*hps-phi*) in *C. glutamicum* to constitute a functional pathway for methanol oxidation and subsequent assimilation of the generated formaldehyde into biomass.

First, the activities of the formaldehyde assimilation modules were evaluated in crude extracts of recombinant *C. glutamicum* strains in *in vitro* enzyme assays. These assays showed that only the Bs(Hps-Phi) module was functionally active in *C. glutamicum* (73 ± 25 mU/mg in the exponential phase [mean ± standard deviation]), whereas only negligible activity (1.4 ± 2 mU/mg) could be detected for the Mg(Hps-Phi) module (Table 2). Consequently, strains expressing the Mg(*hps-phi*) module were not further characterized. The functionality of the methanol oxidation modules was tested by following the methanol oxidation rate of recombinant *C. glutamicum* strains during shake flask cultivations in defined medium containing 55 mM glucose and 120 mM methanol. The strain expressing Cg*adhA* and Bs(*hps-phi*) consumed methanol only slightly faster than the control strain *C. glutamicum*(pVWEx2 pEKEx2) (data not shown). In contrast, the methanol oxidation rate of the recombinant *C. glutamicum* strain expressing Bm(*mdh-act*) and Bs(*hps-phi*) was nearly 3-fold higher (1.3 ± 0.2 mM/h) than in the control strain (0.5 mM/h ± 0.1) (Fig. 2A). Due to these results, we excluded the strain expressing the Cg(*adhA*) module from further experiments and put our focus on the *C. glutamicum* strain expressing the Bm(*mdh-act*) and Bs(*hps-phi*) modules.

Enzyme assays conducted with crude extracts revealed only negligible MDH activity in the exponential growth phase, whereas slightly higher activity was detected in the second growth phase (0.7 ± 0.5 mU/mg) (Table 2). These results were in line with the observation that methanol oxidation was more pronounced in the second growth phase (Fig. 2A). Since IPTG-inducible expression of Bm(*mdh-act*) seems not to be suitable due to the low activity of Bm(Mdh-Act) in the exponential growth phase, we also evaluated the application of a strong constitutive promoter to control heterologous gene expression. For this purpose, the expression of both modules, Bm(*mdh-act*) and Bs(*hps-phi*), was set under the control of the constitutive promoter P*tuf*. Enzyme assays with crude cell extract of the respective strain revealed that the specific MDH activity in the exponential growth phase was significantly increased, from 0.4 ± 0.2 mU/mg to 3.3 ± 1.2 mU/mg (Table 2).

Downloaded from http://aem.asm.org/ on November 19, 2019 by guest

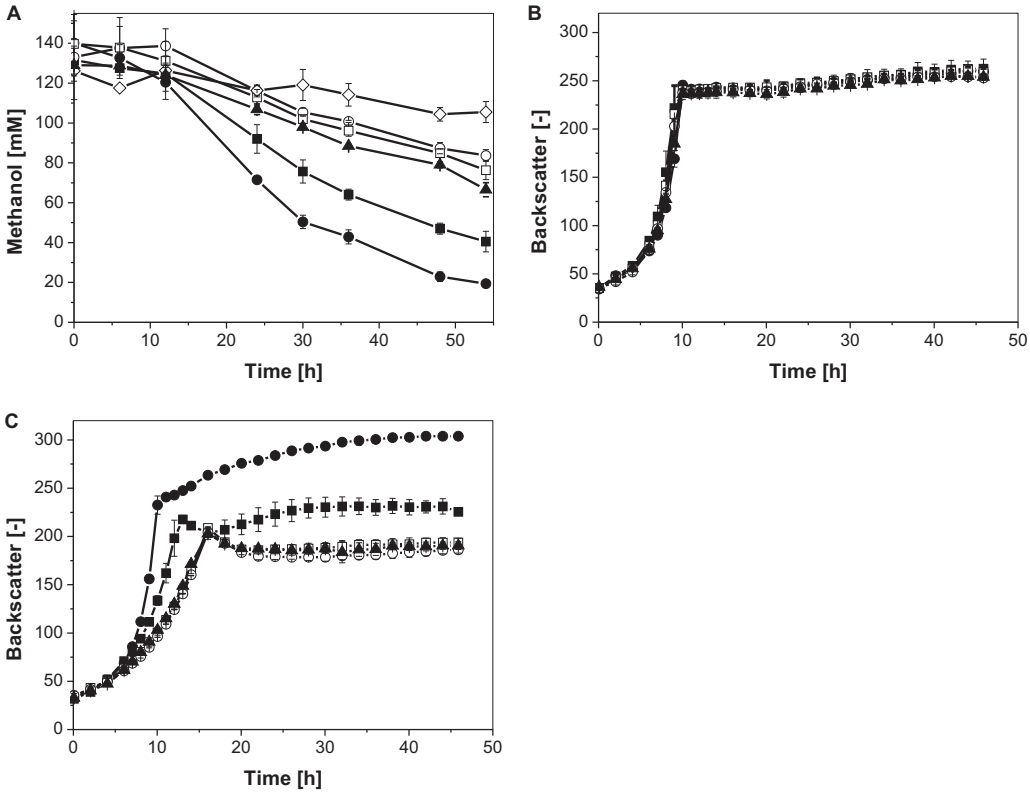

FIG 2 (A) Methanol consumption in CGXII defined medium supplemented with 55 mM glucose and 120 mM methanol. (B) Growth in CGXII defined medium supplemented with 55 mM glucose. (C) Growth in CGXII defined medium supplemented with 55 mM glucose and 120 mM methanol of recombinant *C. glutamicum* strains. Induction of gene expression was achieved with 1.5 mM IPTG in the case of P*tac*-controlled gene expression. Three independent shake-flask experiments, always accompanied by a methanol evaporation control, were performed for the determination of the methanol concentration (◇). Monitoring of growth was performed in 48-well FlowerPlates by using a BioLectorBasic apparatus ($n = 3$). Strains: *C. glutamicum* Bm(*mdh-act*) Bs(*hps-phi*) (■), *C. glutamicum* P*tuf*-Bm(*mdh-act*) P*tuf*-Bs(*hps-phi*) (●), *C. glutamicum* P*tuf*-Bm(*mdh-act*) pEKEx2 (▲), *C. glutamicum* pVWEx2 pEKEx2 (+ IPTG) (□), and *C. glutamicum* pVWEx2 pEKEx2 (- IPTG) (○).

During shake flask experiments for comparing the effect of constitutive and inducible heterologous expression of both modules on methanol consumption, no significant difference was observed in the exponential growth phase. This could be explained by the low biomass at the beginning of the cultivations, leading to only a slow consumption of the supplied methanol in the culture supernatant. These differences could not be reliably distinguished from the background of evaporation of this volatile alcohol. However, over the course of the whole cultivation, a higher average methanol consumption rate (1.7 ± 0.3 mM/h) tha in the strain expressing both modules under the control of the inducible promoter P*tac* (1.3 ± 0.2 mM/h) was obtained (Fig. 2A). In the second growth phase, these results were even more significant. The specific methanol consumption rates for both strains were 6.49 ± 0.4 μM/(h · BS) and 5.78 ± 0.2 μM/(h · BS), respectively.

Initial experiments showed that all recombinant strains and the control strain *C. glutamicum*(pVWEx2 pEKEx2) showed comparable growth behaviors in medium containing 55 mM glucose without methanol (Fig. 2B). In the presence of 120 mM methanol, major differences in growth and final backscatter of the cultures were observed (Fig. 2C). The growth of the control strain and of the recombinant strain expressing the methanol oxidation and formaldehyde assimilation modules under the control of P*tac* were significantly retarded, revealing an inhibitory effect of methanol. The latter strain could cope slightly better with methanol, as it grew faster during the exponential growth phase. However, this growth advantage cannot be explained by the observed higher methanol oxidation of the recombinant strain (1.3 ± 0.2 mM/h) in comparison to the control strain (0.5 ± 0.1 mM/h) during the course of the cultivation, since both strains hardly consumed methanol in the exponential growth phase (Fig. 2A). At the end of the exponential growth phase, backscatter measurements showed a decrease in cell density in both cultures (Fig. 2C). In contrast to the control culture, the *C. glutamicum* Bm(*mdh-act*) Bs(*hps-phi*) culture showed a second growth phase, leading to a significantly (1.3-fold) higher final backscatter (Fig. 2C) and an increased CDW by 4% (Table 3) in comparison to the control strain. The same was observed for a *C. glutamicum* strain that exclusively expressed the methanol oxidation module but not the formaldehyde assimilation module (see Fig. S1 in the supplemental material). This led to the assumption that the observed higher final backscatter of the *C. glutamicum* Bm(*mdh-act*) Bs(*hps-phi*) culture compared to the control strain *C. glutamicum*(pVWEx2 pEKEx2) does not reflect the assimilation of methanol-derived carbon but could be due to a lower methanol concentration in the medium during the second growth phase, thereby diminishing its inhibitory effect.

In contrast, the *C. glutamicum* strain expressing the genes for methanol oxidation and formaldehyde assimilation under the

Downloaded from http://aem.asm.org/ on November 19, 2019 by guest

TABLE 3 Cell dry weight measures for *C. glutamicum* strains[a]

Strain	CDW (mg/ml of culture broth)
Recombinant *C. glutamicum* strains	
Bm(*mdh-act*) Bs(*hps-phi*)	6.72 ± 0.05
P*tuf*-Bm(*mdh-act*) P*tuf*-Bs(*hps-phi*)	8.37 ± 0.03
Control (pVWEx2 pEKEx2)	6.49 ± 0.13
Recombinant *C. glutamicum* Δ*ald* Δ*adhE* strains	
P*tuf*-Bm(*mdh-act*) P*tuf*-Bs(*hps-phi*)	6.75 ± 0.01
P*tuf*-Bm(*mdh3-act*) P*tuf*-Bs(*hps-phi*)	7.14 ± 0.13
P*tuf*-Bm(*mdh-act*) pEKEx2	4.87 ± 0.25
Control (pVWEx2 pEKEx2)	6.35 ± 0.10

[a] Cells were grown in CGXII defined medium containing glucose (55 mM) and methanol (120 mM). The CDW was determined 32 h after inoculation (the second growth phase). Genes under the control of P*tac* were induced with 1.5 mM IPTG at an OD_{600} of 1.0. Means and standard deviations were calculated from triplicates.

control of P*tuf* showed similar growth in defined medium with or without methanol. In comparison to the *C. glutamicum* strain expressing the same genes under the control of P*tac*, higher backscatter of the culture at the end of exponential growth was detected. Moreover, an additional increase of the cell density during the second growth phase in methanol-containing medium was observed that led to a significantly higher final backscatter and to a CDW that was increased by 18% (Table 3). Glucose measurements during cultivation of both strains and of the control strain revealed that glucose was completely consumed at the end of the exponential growth phase. Thus, the metabolization of methanol during this phase appears to be a diauxic shift. Remarkably, *C. glutamicum* P*tuf*-Bm(*mdh-act*) P*tuf*-Bs(*hps-phi*) also grew to a higher final backscatter in the presence of methanol (Fig. 2C) and showed a significantly increased CDW under these conditions (8.4 ± 0.03 versus 8.0 ± 0.05 mg/ml) (Table 3). These results hint toward the ability of this particular *C. glutamicum* strain to convert methanol-derived carbon into biomass. This was verified by analysis of a *C. glutamicum* strain expressing only the genes for methanol oxidation under the control of P*tuf* [*C. glutamicum* P*tuf*-Bm(*mdh-act*(pEKEx2)]. This strain grew slower in the presence of methanol than the control strain, which additionally expressed the genes enabling formaldehyde assimilation.

Methanol-derived carbon is assimilated into intracellular metabolites of *C. glutamicum*. ^{13}C-methanol-labeling experiments were performed to validate that the expression of P*tuf*-Bm(*mdh-act*) and P*tuf*-Bs(*hps-phi*) results in the incorporation of methanol-derived carbon into intracellular metabolites. Two independent batch fermentations were run in CGXII medium supplemented with 55 mM glucose and 120 mM [^{13}C]methanol. Quenching of the metabolic activity as well as analysis of the intracellular metabolites were performed in the exponential growth phase, at the point of transition to the second growth phase, as well as 12 h and 24 h after reaching the second growth phase. In the exponential growth phase, incorporation of [^{13}C]methanol-derived carbon into intracellular metabolites could already be detected, although amounts were quite low (up to 5% labeling fractions in the m + 1 mass isotopomers) (see Fig. S2 in the supplemental material). This showed that small amounts of methanol below the GC detection limit were already oxidized to formaldehyde and subsequently assimilated into biomass in the exponential growth phase. With the transition to the second growth phase,

TABLE 4 Incorporation of [^{13}C]methanol-derived carbon into intracellular metabolites of *C. glutamicum* P*tuf*-Bm(*mdh-act*) P*tuf*-Bs(*hps-phi*)[a]

Metabolite	m + 1 labeled (%)	
	BR1	BR2
Glucose-6-phosphate	2.7	3.6
6-Phosphogluconate	2.0	ND
Sedoheptulose-7-phosphate	6.0	6.2
Fructose-1,6-bisphosphate	8.2	6.2
Dihydroxyacetone phosphate	3.2	3.0
2-/3-Phosphoglycerate	4.0	5.0
Phosphoenolpyruvate	1.9	4.2
Pyruvate	5.6	5.1
α-Ketoglutarate	8.0	8.3
Succinate	8.5	8.7
Histidine	ND	6.9
Serine	6.1	8.5
Homoserine	4.8	4.5
Tryptophan	10.7	9.9
Tyrosine	10.1	9.2
Phenylalanine	7.8	7.8
Valine	6.8	5.7
Alanine	7.0	7.1
Proline	5.6	5.2
Arginine	4.5	3.6
Glutamine	6.0	6.2
Lysine	8.3	7.7
Aspartate	9.3	9.1
Threonine	5.1	6.4

[a] Two independent batch reactors (BR1 and BR2) were run with CGXII defined medium supplemented with 55 mM glucose and 120 mM ^{13}C-labeled methanol. Quenching of the metabolic activity was performed during the transition to the second growth phase. Mass isotopomer measurements were performed for selected metabolites, and the corresponding M + 1 mass traces are listed. Raw mass spectrometry data were corrected for the contribution of all naturally abundant isotopes. ND, not determined.

labeling fractions of 3 to 10% in the m + 1 mass isotopomers of various metabolites, such as organic acids (succinate and α-ketoglutarate) and sugar phosphates (glucose-6-phosphate and fructose-1,6-bisphosphate), as well as amino acids (L-serine and L-lysine), were detected (Table 4). For some metabolites, the labeling fractions in the M + 1 mass isotopomers were increased even after a further 12 h of cultivation (see Fig. S4 in the supplemental material). No ^{13}C-labeling that was higher than the natural ^{13}C abundance was detected in any metabolites of the negative-control, *C. glutamicum*(pVWEx2 pEKEx2) (data not shown). In comparison to this control, a high $^{13}CO_2$/total CO_2 ratio for the strain expressing the methanol oxidation and formaldehyde assimilation modules under the control of P*tuf* was observed (Fig. 3). This led us to the assumption that most of the [^{13}C]methanol-derived formaldehyde is oxidized to $^{13}CO_2$ via the endogenous pathway for formaldehyde dissimilation.

Implementation of methanol oxidation and formaldehyde assimilation in *C. glutamicum* Δ*ald* Δ*adhE*. ^{13}C-methanol-labeling experiments revealed that only a small amount of [^{13}C]methanol-derived carbon was assimilated into biomass precursors of *C. glutamicum* genes for methanol oxidation and formaldehyde assimilation (Table 4). Consequently, P*tuf*-Bm(*mdh-act*) as well as P*tuf*-Bm(*mdh-act*) in combination with P*tuf*-Bs(*hps-phi*) were expressed in *C. glutamicum* Δ*ald* Δ*adhE*, a strain which is strongly impaired in its ability to oxidize formaldehyde to

Downloaded from http://aem.asm.org/ on November 19, 2019 by guest

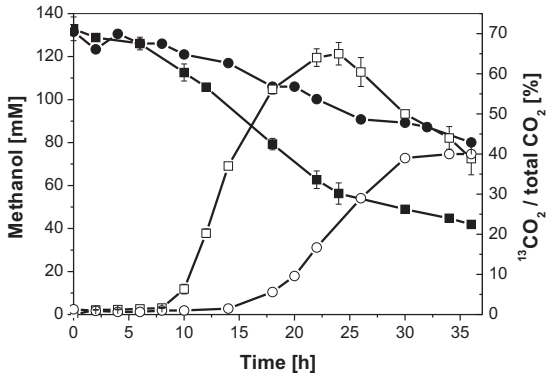

FIG 3 Methanol consumption (filled symbols) and $^{13}CO_2$ formation, reported as the $^{13}CO_2$/total CO_2 ratio (open symbols) of *C. glutamicum* P*tuf*-Bm(*mdh-act*) P*tuf*-Bs(*hps-phi*) (■) and *C. glutamicum* pVWEx2 pEKEx2 (●) during cultivation in CGXII defined medium supplemented with 55 mM glucose and 120 mM ^{13}C-labeled methanol in bioreactors. Two independent experiments were performed, and mean values are shown.

CO_2 (22, 23). This approach should prevent loss of methanol-derived formaldehyde as CO_2 and boost formaldehyde assimilation. In addition, *C. glutamicum* Δ*ald* Δ*adhE*(pVWEx2 pEKEx2), only harboring the empty plasmids, was constructed as a control. All strains were analyzed regarding growth and methanol consumption in the presence of methanol to check if the absence of the "safety valve" for formaldehyde oxidation affected growth.

Determination of the *in vitro* enzyme activities revealed that all enzymes were functionally active in recombinant *C. glutamicum* Δ*ald* Δ*adhE* strains (Table 2). In glucose-containing medium, growth of all strains was similar (Fig. 4B) and comparable to that of the strains constructed on the basis of wild-type *C. glutamicum* (Fig. 2B). In comparison, *C. glutamicum* Δ*ald* Δ*adhE*(pVWEx2 pEKEx2) displayed retarded growth and a 33% reduced final backscatter in the presence of methanol. The *C. glutamicum* Δ*ald* Δ*adhE* strain expressing only P*tuf*-Bm(*mdh-act*) showed even slower growth in the presence of methanol, and the final backscatter of the culture was reduced by an additional 35% (Fig. 4C). The methanol consumption rate was as low as that observed for the control strain (0.52 ± 0.1 mM/h) (Fig. 4A). This strain possesses the heterologous methanol dehydrogenase for oxidation of methanol to formaldehyde, but due to the absence of Bs(Hps-Phi) and the lack of Ald and AdhE, the toxic accumulation of formaldehyde cannot be avoided, neither via assimilation by the RuMP pathway nor via dissimilation to CO_2. However, quantification of intracellular formaldehyde was not successful.

The *C. glutamicum* Δ*ald* Δ*adhE* strain possessing the methanol oxidation module [P*tuf*-Bm(*mdh-act*)] and the formaldehyde assimilation module [P*tuf*-Bs(*hps-phi*)] showed an increased methanol oxidation rate (1.25 ± 0.2 mM/h) in comparison to the con-

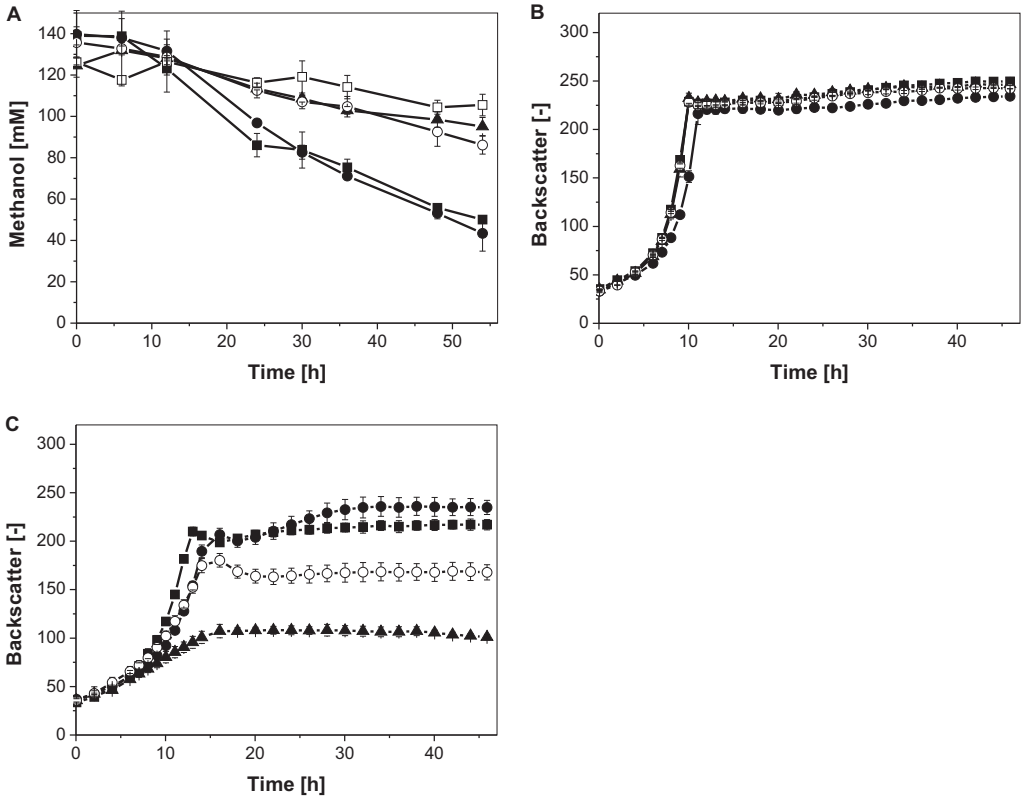

FIG 4 (A) Methanol consumption in CGXII defined medium supplemented with 55 mM glucose and 120 mM methanol. (B) Growth in CGXII defined medium supplemented with 55 mM glucose. (C) Growth in CGXII defined medium supplemented with 55 mM glucose and 120 mM methanol of recombinant *C. glutamicum* Δ*ald* Δ*adhE* strains. Three independent shake-flask experiments, always accompanied by a methanol evaporation control, were performed for the determination of the methanol concentration (◇). Monitoring of growth was performed in 48-well FlowerPlates by using a BioLectorBasic apparatus ($n = 3$). Strains: *C. glutamicum* Δ*ald* Δ*adhE* P*tuf*-Bm(*mdh-act*) P*tuf*-Bs(*hps-phi*) (■), *C. glutamicum* P*tuf*-Bm(*mdh3-act*) P*tuf*-Bs(*hps-phi*) (●), *C. glutamicum* Δ*ald* Δ*adhE* P*tuf*-Bm(*mdh-act*) pEKEx2 (▲), and *C. glutamicum* Δ*ald* Δ*adhE* pVWEx2 pEKEx2 (○).

Downloaded from http://aem.asm.org/ on November 19, 2019 by guest

trol strain. The specific methanol consumption rate in the second growth phase for this strain was 5.95 ± 0.3 μM/(h · BS) and for the control strain only 3.25 ± 0.2 μM/(h · BS).

Apparently, the recombinant *C. glutamicum* Δ*ald* Δ*adhE* strain had a growth advantage over the control strain in the presence of methanol, since the backscatter was found to be 15% higher at the end of the exponential growth phase. This was also reflected by a higher final CDW (6.75 ± 0.00 mg/ml and 4.87 ± 0.25 mg/ml, respectively). In contrast to *C. glutamicum* P*tuf*-Bm(*mdh-act*) P*tuf*-Bs(*hps-phi*), the recombinant *C. glutamicum* Δ*ald* Δ*adhE* strain did not grow in methanol-containing medium as fast as in medium without methanol, and the final backscatter of the culture was not increased in the presence of methanol.

Finally, we also evaluated Mdh3, the other MDH of *B. methanolicus*, in the *C. glutamicum* Δ*ald* Δ*adhE* strain background. P*tuf*-controlled expression of *mdh3* and *act* in combination with P*tuf*-Bs(*hps-phi*) and cultivation in glucose- and methanol-containing medium revealed methanol consumption, which was similar to the that of *C. glutamicum* Δ*ald* Δ*adhE* P*tuf*-Bm(*mdh-act*) P*tuf*-Bs(*hps-phi*) (Fig. 4A). However, with this strain, a slightly higher final backscatter of the culture and an increased CDW was reached (Fig. 4B; Table 3).

Increased assimilation of methanol-derived carbon by *C. glutamicum* Δ*ald* Δ*adhE*. ^{13}C-methanol-labeling experiments were performed to answer the question whether the elimination of the endogenous pathway for formaldehyde dissimilation results in increased assimilation of methanol-derived carbon into the biomass, although the determined overall biomass yield was not higher in the presence of methanol. In addition, methanol consumption and generation of $^{13}CO_2$ was measured (see Fig. S3A and B in the supplemental material). Already in the exponential growth phase, incorporation of [^{13}C]methanol-derived carbon into intracellular metabolites of *C. glutamicum* Δ*ald* Δ*adhE* P*tuf*-Bm(*mdh-act*) P*tuf*-Bs(*hps-phi*) and of *C. glutamicum* Δ*ald* Δ*adhE* P*tuf*-Bm(*mdh3-act*) P*tuf*-Bs(*hps-phi*) was observed. Labeling fractions of up to 11% in the m + 1 mass isotopomers were detected. With the entrance to the second growth phase, the labeling fractions were found to be about 3-fold higher than the wild-type *C. glutamicum* strain expressing the methanol oxidation and formaldehyde assimilation modules (Table 4; Fig. 5). For the *C. glutamicum* Δ*ald* Δ*adhE* strain expressing P*tuf*-Bm(*mdh3-act*) and P*tuf*-Bs(*hps-phi*), an average increase of 10% of the labeling fractions in the m + 1 mass isotopomers of intracellular metabolites was observed (see Fig. S4 and S5 in the supplemental material).

DISCUSSION

Only few methylotrophic organisms, such as *B. methanolicus* and *M. extorquens*, have been engineered to produce biotechnologically interesting compounds from methanol (49–51). In this study, we followed the opposite strategy by engineering the nonmethylotrophic platform organism *C. glutamicum* to utilize methanol instead of turning a methylotrophic organism into a production strain.

The wild-type *C. glutamicum* is already able to oxidize methanol, predominantly catalyzed by the alcohol dehydrogenase AdhA (22). Nonetheless, we evaluated the implementation of the NAD^+-dependent methanol dehydrogenase from *B. methanolicus* for increasing the methanol oxidation rate. Since wild-type *C. glutamicum* already possesses an endogenous pathway for the detoxification of naturally occurring cytotoxic formaldehyde to CO_2 (22, 23), only a pathway for assimilation of formaldehyde into biomass was required. Heterologous expression of genes for HPS and PHI from methylotrophic organisms, both key enzymes of the RuMP) pathway, has already been performed to confer the capability of formaldehyde assimilation to *Burkholderia cepacia* and *Pseudomonas putida*, respectively (20, 52, 53). Surprisingly, in this study heterologous expression of *hps* and *phi* from the methylotroph bacterium *M. gastri*, which is closely related to *C. glutamicum*, did not result in active enzymes. As an alternative, we tried the expression of *hps* and *phi* of *B. subtilis*, which requires these genes only for formaldehyde detoxification (52, 54), and we were able to complete a functional RuMP pathway in *C. glutamicum*.

Functional expression of the modules for methanol oxidation [Bm(Mdh-Act)] and formaldehyde assimilation [Bs(Hps-Phi)] in wild-type *C. glutamicum*, as well as the selection of a suitable promoter for gene expression (P*tuf*), resulted in a 3-fold-increased methanol oxidation rate (1.7 ± 0.2 mM/h) in comparison to the *C. glutamicum*(pVWEx2 pEKEx2) control strain (0.5 ± 0.1 mM/h). Furthermore, the inhibitory effects of methanol on growth and biomass formation of this control strain could be compensated by *C. glutamicum* P*tuf*-Bm(*mdh-act*) P*tuf*-Bs(*hps-phi*). This strain showed the same growth in medium with and without methanol. Furthermore, at the end of the exponential growth phase, a higher backscatter than with the control strain was observed. This effect could be explained by the generation of additional NADH due to the methanol dehydrogenase-catalyzed oxidation of methanol in the exponential growth phase and subsequent generation of ATP via oxidative phosphorylation. Thus, less glucose has to be dissimilated for energy generation and can be used for synthesis of biomass precursors. This effect on biomass formation was also observed during coutilization of formate with glucose by *Candida utilis* and *Penicillium chrysogenum* (55, 56), as well as during coutilization of formaldehyde with glucose by *Saccharomyces cerevisiae* expressing a formaldehyde dehydrogenase and a formate dehydrogenase from *Hansenula polymorpha* (57). Furthermore, the increased biomass formation in recombinant *C. glutamicum* strains could also be explained by assimilation of methanol-derived formaldehyde via HPS- and PHI-catalyzed reactions. Indeed, [^{13}C]methanol-labeling experiments revealed up to 5% labeling fractions in the m + 1 mass isotopomers of various intracellular metabolites in samples taken from the exponential growth phase.

After exponential growth in glucose-methanol medium, recombinant *C. glutamicum* cells seem to enter a second growth phase, represented by slowly increasing backscatter and an increased CDW (8.4 ± 0.03 mg/ml versus 8.0 ± 0.05 mg/ml in medium without methanol). Again, [^{13}C]methanol-labeling experiments showed 3 to 10% m + 1 labeling of intracellular metabolites, indicating assimilation of methanol-derived carbon into biomass. However, *C. glutamicum* P*tuf*-Bm(*mdh-act*) P*tuf*-Bs(*hps-phi*) consumed about 40% more methanol and produced 31% more CO_2 than did *C. glutamicum*(pVWEx2 pEKEx2) when we calculated the amounts until the respective maximal CO_2 production was reached. This means that most of the consumed methanol (about 78%) in the recombinant strain is oxidized to CO_2 via the endogenous pathway for formaldehyde oxidation and not assimilated via the RuMP pathway. Since implementation of the modules for methanol oxidation and formaldehyde assimilation in wild-type *C. glutamicum* resulted in a high flux toward CO_2 formation, we also engineered *C. glutamicum* Δ*ald* Δ*adhE*, a strain severely impaired in its ability to detoxify formaldehyde, for assimilation of methanol. As observed for recombinant wild-type *C.*

Downloaded from http://aem.asm.org/ on November 19, 2019 by guest

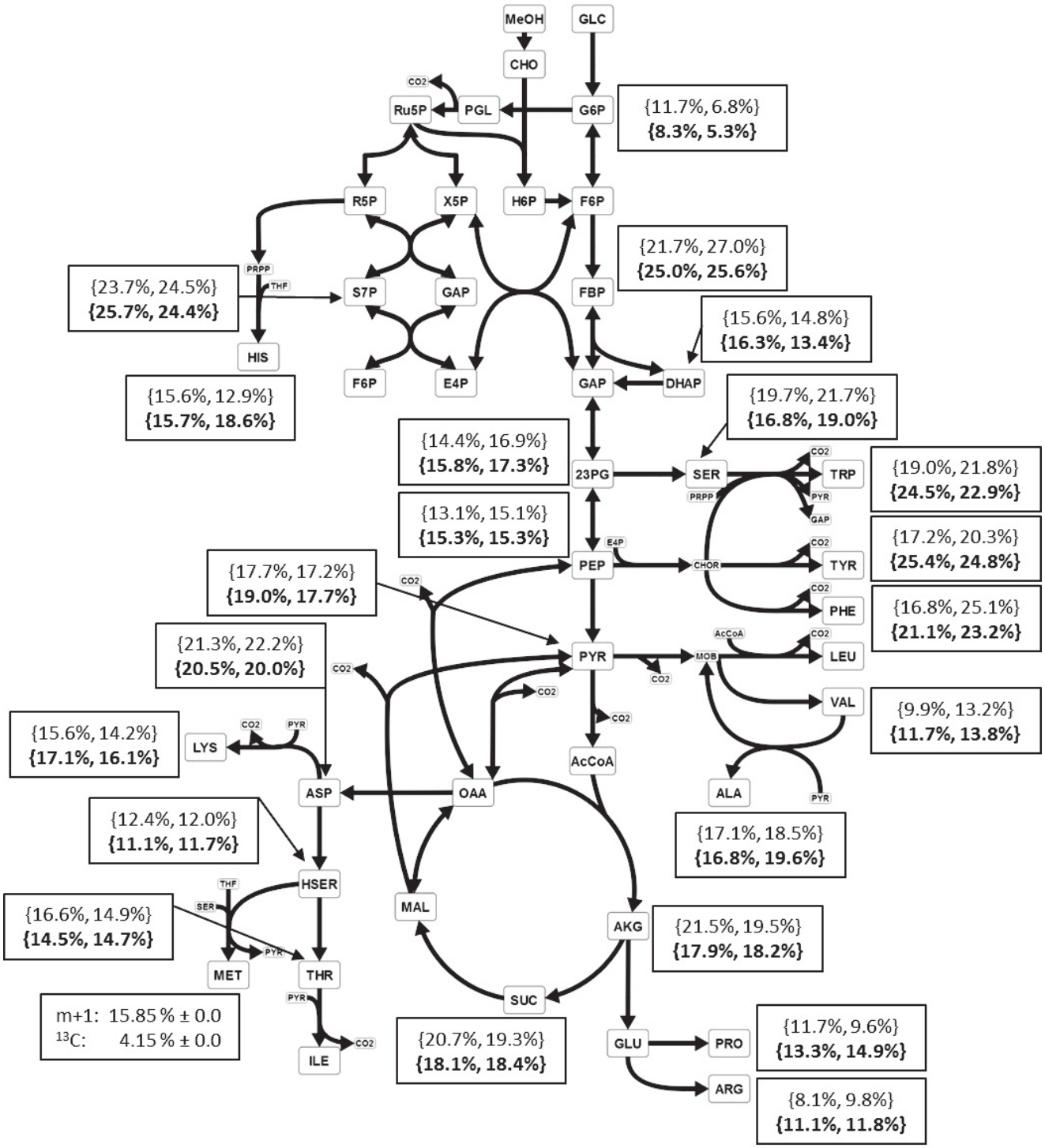

FIG 5 Simplified overview of the central carbon metabolism, including the oxidation of methanol via Bm(Mdh-Act) or Bm(Mdh3-Act) and the assimilation of formaldehyde via the RuMP pathway of recombinant *C. glutamicum* Δ*ald* Δ*adhE* strains. Additionally, the labeling fractions of the M + 1 mass isotopomers of the measured intracellular metabolites are listed for *C. glutamicum* Δ*ald* Δ*adhE* P*tuf*-Bm(*mdh-act*) P*tuf*-Bs(*hps-phi*) (values in the upper row) and *C. glutamicum* Δ*ald* Δ*adhE* P*tuf*-Bm(*mdh3-act*) P*tuf*-Bs(*hps-phi*) (values in the lower row, bold). For each strain, two independent batch reactors (BR1 and BR2) with CGXII defined medium (55 mM glucose, 120 mM ^{13}C-labeled methanol) were run. Quenching of metabolic activity as well as intracellular metabolic analysis were performed at the transition to the second growth phase, and raw mass spectrometry data were corrected for the contribution of all naturally abundant isotopes. Abbreviations: amino acids are presented according to their 3-letter standard abbreviations; MeOH, methanol; GLC, glucose; CHO, formaldehyde; G6P, glucose-6-phosphate; PGL, phosphogluconolactone; Ru5P, ribulose-5-phosphate; R5P, ribose-5-phosphate; X5P, xylulose-5-phosphate; S7P, sedoheptulose-7-phosphate; E4P, erythrosee-4-phosphate; H6P, hexulose-6-phosphate; F6P, fructose-6-phosphate; FBP, fructose-1,6-bisphosphate; GAP, glyceraldehyde-3-phosphate; DHAP, dihydroxyacetone phosphate; 23PG, 2-/3-phosphoglycerate; PEP, phosphoenolpyruvate; PYR, pyruvate; AcCoA, acetyl coenzyme A; AKG, α-ketoglutarate; SUC, succinate; MAL, malate; OAA, oxaloacetate; THF, tetrahydrofuran; PRPP, phosphoribosyl pyrophosphate; CHOR, chorismate.

Downloaded from http://aem.asm.org/ on November 19, 2019 by guest

glutamicum strains, the implementation of the modules for methanol oxidation, [P*tuf*-Bm(*mdh-act*)] or [P*tuf*-Bm(*mdh3-act*)], and formaldehyde assimilation [P*tuf*-Bs(*hps-phi*)] in *C. glutamicum* Δ*ald* Δ*adhE* resulted in a 15% higher backscatter at the end of the exponential growth phase in methanol-containing medium compared to *C. glutamicum* Δ*ald* Δ*adhE*(pVWEx2 pEKEx2). As discussed before, this effect might be due to the generation of additional NADH during methanol oxidation. However, in contrast to recombinant wild-type *C. glutamicum* strains, oxidation of methanol in recombinant *C. glutamicum* Δ*ald* Δ*adhE* is accompanied by channeling of more methanol-derived formaldehyde into the synthetic RuMP cycle, because *C. glutamicum* Δ*ald* Δ*adhE* does not have the "safety valve" for formaldehyde detoxification to CO_2. Without the assimilation of formaldehyde, toxic amounts of this intermediate would accumulate and inhibit cell growth. Previously, we showed that 4 mM formaldehyde completely inhibited cell growth of *C. glutamicum* (22). Indeed, [^{13}C]methanol-labeling experiments revealed that the M + 1 labeling of intracellular metabolites in the exponential growth phase was doubled in comparison to the wild-type *C. glutamicum* strain expressing the same genes; in the transition to the second growth phase, it was even higher (3-fold higher). However, elimination of the "safety valve" also led to a reduced methanol consumption rate, retarded growth, and a lowered final CDW, most probably due to accumulation of formaldehyde. Possibly, synthetic formaldehyde assimilation is currently not efficient enough to keep the intracellular formaldehyde concentrations below the toxicity threshold.

In summary, for the first time *C. glutamicum* was engineered to utilize methanol as a carbon and energy source during growth in sugar-based defined medium. Furthermore, detection of ^{13}C-labeled amino acids indicates that methanol can also be used as an auxiliary substrate for the production of these value-added compounds. For a more efficient use of methanol during sugar-based fermentation processes, methanol oxidation to formaldehyde has to be increased, whereas accumulation of toxic formaldehyde has to be minimized. Thus, future experiments should aim at balancing the synthetic formaldehyde assimilation and the endogenous dissimilation. This could be achieved by metabolic engineering or by employing process engineering strategies, e.g., by developing a fed-batch process with continuous methanol feeding. This would ensure constant methanol availability during the cultivation, as has been already realized for *B. methanolicus* MGA3 (21, 58).

ACKNOWLEDGMENTS

Sabrina Witthoff is an associated fellow of the CLIB-Graduate Cluster Industrial Biotechnology.

We thank Meike Baumgart (Forschungszentrum Jülich) for carefully reading the manuscript and Petra Geilenkirchen (Forschungszentrum Jülich) for the LC tandem MS measurements.

REFERENCES

1. **Becker J, Wittmann C.** 2012. Bio-based production of chemicals, materials and fuels: *Corynebacterium glutamicum* as versatile cell factory. Curr Opin Biotechnol **23:**631–640. http://dx.doi.org/10.1016/j.copbio.2011.11.012.
2. **Okino S, Noburyu R, Suda M, Jojima T, Inui M, Yukawa H.** 2008. An efficient succinic acid production process in a metabolically engineered *Corynebacterium glutamicum* strain. Appl Microbiol Biotechnol **81:**459–464. http://dx.doi.org/10.1007/s00253-008-1668-y.
3. **Litsanov B, Brocker M, Bott M.** 2012. Toward homosuccinate fermentation: metabolic engineering of *Corynebacterium glutamicum* for anaerobic production of succinate from glucose and formate. Appl Environ Microbiol **78:**3325–3337. http://dx.doi.org/10.1128/AEM.07790-11.
4. **Wieschalka S, Blombach B, Bott M, Eikmanns BJ.** 2013. Bio-based production of organic acids with *Corynebacterium glutamicum*. Microb Biotechnol **6:**87–102. http://dx.doi.org/10.1111/1751-7915.12013.
5. **Schneider J, Wendisch VF.** 2011. Biotechnological production of polyamines by bacteria: recent achievements and future perspectives. Appl Microbiol Biotechnol **91:**17–30. http://dx.doi.org/10.1007/s00253-011-3252-0.
6. **Mimitsuka T, Sawai H, Hatsu M, Yamada K.** 2007. Metabolic engineering of *Corynebacterium glutamicum* for cadaverine fermentation. Biosci Biotechnol Biochem **71:**2130–2135. http://dx.doi.org/10.1271/bbb.60699.
7. **Kind S, Wittmann C.** 2011. Bio-based production of the platform chemical 1,5-diaminopentane. Appl Microbiol Biotechnol **91:**1287–1296. http://dx.doi.org/10.1007/s00253-011-3457-2.
8. **Inui M, Kawaguchi H, Murakami S, Vertes AA, Yukawa H.** 2004. Metabolic engineering of *Corynebacterium glutamicum* for fuel ethanol production under oxygen-deprivation conditions. J Mol Microbiol Biotechnol **8:**243–254. http://dx.doi.org/10.1159/000086705.
9. **Smith KM, Cho KM, Liao JC.** 2010. Engineering *Corynebacterium glutamicum* for isobutanol production. Appl Microbiol Biotechnol **87:**1045–1055. http://dx.doi.org/10.1007/s00253-010-2522-6.
10. **Blombach B, Riester T, Wieschalka S, Ziert C, Youn JW, Wendisch VF, Eikmanns BJ.** 2011. *Corynebacterium glutamicum* tailored for efficient isobutanol production. Appl Environ Microbiol **77:**3300–3310. http://dx.doi.org/10.1128/AEM.02972-10.
11. **Zahoor A, Lindner SN, Wendisch VF.** 2012. Metabolic engineering of *Corynebacterium glutamicum* aimed at alternative carbon sources and new products. Comput Struct Biotechnol J **3:**e201210004. http://dx.doi.org/10.5936/csbj.201210004.
12. **Kelle R, Hermann T, Bathe B.** 2005. Lysine production, p 467–490. *In* Eggeling L, Bott M (ed), Handbook of *Corynebacterium glutamicum*. CRC Press, Boca Raton, FL.
13. **Kimura E.** 2005. Glutamate production, p 441–465. *In* Eggeling L, Bott M (ed), Handbook of *Corynebacterium glutamicum*. CRC Press, Boca Raton, FL.
14. **Schrader J, Schilling M, Holtmann D, Sell D, Filho MV, Marx A, Vorholt JA.** 2009. Methanol-based industrial biotechnology: current status and future perspectives of methylotrophic bacteria. Trends Biotechnol **27:**107–115. http://dx.doi.org/10.1016/j.tibtech.2008.10.009.
15. **Uhde A, Youn JW, Maeda T, Clermont L, Matano C, Krämer R, Wendisch VF, Seibold GM, Marin K.** 2013. Glucosamine as carbon source for amino acid-producing *Corynebacterium glutamicum*. Appl Microbiol Biotechnol **97:**1679–1687. http://dx.doi.org/10.1007/s00253-012-4313-8.
16. **Olah GA, Prakash GK, Goeppert A, Czaun M, Mathew T.** 2013. Self-sufficient and exclusive oxygenation of methane and its source materials with oxygen to methanol via metgas using oxidative bi-reforming. J Am Chem Soc **135:**10030–10031. http://dx.doi.org/10.1021/ja405439c.
17. **Olah GA, Goeppert A, Czaun M, Prakash GK.** 2013. Bi-reforming of methane from any source with steam and carbon dioxide exclusively to metgas (CO_2-H_2) for methanol and hydrocarbon synthesis. J Am Chem Soc **135:**648–650. http://dx.doi.org/10.1021/ja311796n.
18. **Wesselbaum S, Vom Stein T, Klankermayer J, Leitner W.** 2012. Hydrogenation of carbon dioxide to methanol by using a homogeneous ruthenium-phosphine catalyst. Angew Chem Int Ed Engl **51:**7499–7502. http://dx.doi.org/10.1002/anie.201202320.
19. **Law K, Rosenfeld J, Jackson M.** 2013. Methanol as a renewable energy resource. Tiax LLC, Cupertino, CA.
20. **Koopman FW, de Winde JH, Ruijssenaars HJ.** 2009. C_1 compounds as auxiliary substrate for engineered *Pseudomonas putida* S12. Appl Microbiol Biotechnol **83:**705–713. http://dx.doi.org/10.1007/s00253-009-1922-y.
21. **Brautaset T, Jakobsen OM, Josefsen KD, Flickinger MC, Ellingsen TE.** 2007. *Bacillus methanolicus*: a candidate for industrial production of amino acids from methanol at 50°C. Appl Microbiol Biotechnol **74:**22–34. http://dx.doi.org/10.1007/s00253-006-0757-z.
22. **Witthoff S, Mühlroth A, Marienhagen J, Bott M.** 2013. C_1 metabolism in *Corynebacterium glutamicum*: an endogenous pathway for oxidation of methanol to carbon dioxide. Appl Environ Microbiol **79:**6974–6983. http://dx.doi.org/10.1128/AEM.02705-13.
23. **Lessmeier L, Hoefener M, Wendisch VF.** 2013. Formaldehyde degradation in *Corynebacterium glutamicum* involves acetaldehyde dehydroge-

Downloaded from http://aem.asm.org/ on November 19, 2019 by guest

nase and mycothiol-dependent formaldehyde dehydrogenase. Microbiology **159:**2651–2662. http://dx.doi.org/10.1099/mic.0.072413-0.
24. **Nakagawa T, Mitsui R, Tani A, Sasa K, Tashiro S, Iwama T, Hayakawa T, Kawai K.** 2012. A catalytic role of XoxF1 as La^{3+}-dependent methanol dehydrogenase in *Methylobacterium extorquens* strain AM1. PLoS One **7:**e50480. http://dx.doi.org/10.1371/journal.pone.0050480.
25. **Arfman N, Watling EM, Clement W, van Oosterwijk RJ, de Vries GE, Harder W, Attwood MM, Dijkhuizen L.** 1989. Methanol metabolism in thermotolerant methylotrophic *Bacillus* strains involving a novel catabolic NAD-dependent methanol dehydrogenase as a key enzyme. Arch Microbiol **152:**280–288. http://dx.doi.org/10.1007/BF00409664.
26. **Vorholt JA.** 2002. Cofactor-dependent pathways of formaldehyde oxidation in methylotrophic bacteria. Arch Microbiol **178:**239–249. http://dx.doi.org/10.1007/s00203-002-0450-2.
27. **Yurimoto H, Kato N, Sakai Y.** 2005. Assimilation, dissimilation, and detoxification of formaldehyde, a central metabolic intermediate of methylotrophic metabolism. Chem Rec **5:**367–375. http://dx.doi.org/10.1002/tcr.20056.
28. **Chistoserdova L.** 2011. Modularity of methylotrophy, revisited. Environ Microbiol **13:**2603–2622. http://dx.doi.org/10.1111/j.1462-2920.2011.02464.x.
29. **Kato N, Yurimoto H, Thauer RK.** 2006. The physiological role of the ribulose monophosphate pathway in bacteria and archaea. Biosci Biotechnol Biochem **70:**10–21. http://dx.doi.org/10.1271/bbb.70.10.
30. **Sambrook J, Fritsch EF, Maniatis T.** 1989. Molecular cloning: a laboratory manual, 3rd ed. Cold Spring Harbor Laboratory Press, Cold Spring Harbor, NY.
31. **Frunzke J, Engels V, Hasenbein S, Gätgens C, Bott M.** 2008. Co-ordinated regulation of gluconate catabolism and glucose uptake in *Corynebacterium glutamicum* by two functionally equivalent transcriptional regulators, GntR1 and GntR2. Mol Microbiol **67:**305–322. http://dx.doi.org/10.1111/j.1365-2958.2007.06020.x.
32. **Rohe P, Venkanna D, Kleine B, Freudl R, Oldiges M.** 2012. An automated workflow for enhancing microbial bioprocess optimization on a novel microbioreactor platform. Microb Cell Fact **11:**144. http://dx.doi.org/10.1186/1475-2859-11-144.
33. **Radek A, Krumbach K, Gätgens J, Wendisch VF, Wiechert W, Bott M, Noack S, Marienhagen J.** 2014. Engineering of *Corynebacterium glutamicum* for minimized carbon loss during utilization of D-xylose-containing substrates. J Biotechnol **192:**156–160. http://dx.doi.org/10.1016/j.jbiotec.2014.09.026.
34. **Hanahan D.** 1983. Studies on transformation of *Escherichia coli* with plasmids. J Mol Biol **166:**557–580. http://dx.doi.org/10.1016/S0022-2836(83)80284-8.
35. **van der Rest ME, Lange C, Molenaar D.** 1999. A heat shock following electroporation induces highly efficient transformation of *Corynebacterium glutamicum* with xenogeneic plasmid DNA. Appl Microbiol Biotechnol **52:**541–545. http://dx.doi.org/10.1007/s002530051557.
36. **Abe S, Takayama K, Kinoshita S.** 1967. Taxonomical studies on glutamic acid producing bacteria. J Gen Appl Microbiol **13:**279–301. http://dx.doi.org/10.2323/jgam.13.279.
37. **Eikmanns BJ, Kleinertz E, Liebl W, Sahm H.** 1991. A family of *Corynebacterium glutamicum-Escherichia coli* shuttle vectors for cloning, controlled gene-expression, and promoter probing. Gene **102:**93–98. http://dx.doi.org/10.1016/0378-1119(91)90545-M.
38. **Wendisch VF.** 1997. Ph.D. thesis. Heinrich-Heine University, Düsseldorf, Germany.
39. **Witthoff S, Eggeling L, Bott M, Polen T.** 2012. *Corynebacterium glutamicum* harbours a molybdenum cofactor-dependent formate dehydrogenase which alleviates growth inhibition in the presence of formate. Microbiology **158:**2428–2439. http://dx.doi.org/10.1099/mic.0.059196-0.
40. **Bradford MM.** 1976. A rapid and sensitive method for the quantitation of microgram quantities of protein utilizing the principle of protein-dye binding. Anal Biochem **72:**248–254. http://dx.doi.org/10.1016/0003-2697(76)90527-3.
41. **Hektor HJ, Kloosterman H, Dijkhuizen L.** 2002. Identification of a magnesium-dependent NAD(P)(H)-binding domain in the nicotinoprotein methanol dehydrogenase from *Bacillus methanolicus*. J Biol Chem **277:**46966–46973. http://dx.doi.org/10.1074/jbc.M207547200.
42. **Arfman N, Bystrykh L, Govorukhina NI, Dijkhuizen L.** 1990. 3-Hexulose-6-phosphate synthase from thermotolerant methylotroph *Bacillus* C1. Methods Enzymol **188:**391–397. http://dx.doi.org/10.1016/0076-6879(90)88062-F.
43. **Nudelman A, Levovich I, Cutts SM, Phillips DR, Rephaeli A.** 2005. The role of intracellularly released formaldehyde and butyric acid in the anticancer activity of acyloxyalkyl esters. J Med Chem **48:**1042–1054. http://dx.doi.org/10.1021/jm049428p.
44. **van Ooyen J, Noack S, Bott M, Reth A, Eggeling L.** 2012. Improved L-lysine production with *Corynebacterium glutamicum* and systemic insight into citrate synthase flux and activity. Biotechnol Bioeng **109:**2070–2081. http://dx.doi.org/10.1002/bit.24486.
45. **Millard P, Letisse F, Sokol S, Portais JC.** 2012. IsoCor: correcting MS data in isotope labeling experiments. Bioinformatics **28:**1294–1296. http://dx.doi.org/10.1093/bioinformatics/bts127.
46. **Shen YQ, Bonnot F, Imsand EM, RoseFigura JM, Sjolander K, Klinman JP.** 2012. Distribution and properties of the genes encoding the biosynthesis of the bacterial cofactor, pyrroloquinoline quinone. Biochemistry **51:**2265–2275. http://dx.doi.org/10.1021/bi201763d.
47. **Heggeset TM, Krog A, Balzer S, Wentzel A, Ellingsen TE, Brautaset T.** 2012. Genome sequence of thermotolerant *Bacillus methanolicus*: features and regulation related to methylotrophy and production of L-lysine and L-glutamate from methanol. Appl Environ Microbiol **78:**5170–5181. http://dx.doi.org/10.1128/AEM.00703-12.
48. **Krog A, Heggeset TM, Müller JE, Kupper CE, Schneider O, Vorholt JA, Ellingsen TE, Brautaset T.** 2013. Methylotrophic *Bacillus methanolicus* encodes two chromosomal and one plasmid born NAD^+ dependent methanol dehydrogenase paralogs with different catalytic and biochemical properties. PLoS One **8:**e59188. http://dx.doi.org/10.1371/journal.pone.0059188.
49. **Brautaset T, Jakobsen OM, Degnes KF, Netzer R, Naerdal I, Krog A, Dillingham R, Flickinger MC, Ellingsen TE.** 2010. *Bacillus methanolicus* pyruvate carboxylase and homoserine dehydrogenase I and II and their roles for L-lysine production from methanol at 50°C. Appl Microbiol Biotechnol **87:**951–964. http://dx.doi.org/10.1007/s00253-010-2559-6.
50. **Mokhtari-Hosseini ZB, Vasheghani-Farahani E, Heidarzadeh-Vazifekhoran A, Shojaosadati SA, Karimzadeh R, Khosravi Darani K.** 2009. Statistical media optimization for growth and PHB production from methanol by a methylotrophic bacterium. Bioresour Technol **100:**2436–2443. http://dx.doi.org/10.1016/j.biortech.2008.11.024.
51. **Orita I, Nishikawa K, Nakamura S, Fukui T.** 2014. Biosynthesis of polyhydroxyalkanoate copolymers from methanol by *Methylobacterium extorquens* AM1 and the engineered strains under cobalt-deficient conditions. Appl Microbiol Biotechnol **98:**3715–3725. http://dx.doi.org/10.1007/s00253-013-5490-9.
52. **Mitsui R, Kusano Y, Yurimoto H, Sakai Y, Kato N, Tanaka M.** 2003. Formaldehyde fixation contributes to detoxification for growth of a nonmethylotroph, Burkholderia cepacia TM1, on vanillic acid. Appl Environ Microbiol **69:**6128–6132. http://dx.doi.org/10.1128/AEM.69.10.6128-6132.2003.
53. **Yurimoto H, Kato N, Sakai Y.** 2009. Genomic organization and biochemistry of the ribulose monophosphate pathway and its application in biotechnology. Appl Microbiol Biotechnol **84:**407–416. http://dx.doi.org/10.1007/s00253-009-2120-7.
54. **Yasueda H, Kawahara Y, Sugimoto S.** 1999. *Bacillus subtilis yckG* and *yckF* encode two key enzymes of the ribulose monophosphate pathway used by methylotrophs, and *yckH* is required for their expression. J Bacteriol **181:**7154–7160.
55. **Bruinenberg PM, Jonker R, Vandijken JP, Scheffers WA.** 1985. Utilization of formate as an additional energy-source by glucose-limited chemostat cultures of *Candida utilis* Cbs-621 and *Saccharomyces cerevisiae* Cbs-8066: evidence for the absence of transhydrogenase activity in yeasts. Arch Microbiol **142:**302–306. http://dx.doi.org/10.1007/BF00693408.
56. **Harris DM, van der Krogt ZA, van Gulik WM, van Dijken JP, Pronk JT.** 2007. Formate as an auxiliary substrate for glucose-limited cultivation of *Penicillium chrysogenum*: impact on penicillin G production and biomass yield. Appl Environ Microbiol **73:**5020–5025. http://dx.doi.org/10.1128/AEM.00093-07.
57. **Baerends RJ, de Hulster E, Geertman JM, Daran JM, van Maris AJ, Veenhuis M, van der Klei IJ, Pronk JT.** 2008. Engineering and analysis of a *Saccharomyces cerevisiae* strain that uses formaldehyde as an auxiliary substrate. Appl Environ Microbiol **74:**3182–3188. http://dx.doi.org/10.1128/AEM.02858-07.
58. **Pluschkell SB, Flickinger MC.** 2002. Dissimilation of [^{13}C]methanol by continuous cultures of *Bacillus methanolicus* MGA3 at 50°C studied by ^{13}C NMR and isotope-ratio mass spectrometry. Microbiology **148:**3223–3233.

Downloaded from http://aem.asm.org/ on November 19, 2019 by guest